AGU100 ADVANCING EARTH AND SPACE SCIENCE

Geophysical Research Letters

RESEARCH LETTER
10.1029/2018GL077616

Key Points:
- We collected 736 hr of time-lapse footage documenting the evolution of snow bedforms in the Colorado Front Range
- We built and tested classifiers that predict bedform presence as a function of weather
- Bedform and sastrugi presence is best predicted by time since snowfall, instantaneous wind speeds, and maximum wind speeds

Supporting Information:
- Supporting Information S1
- Data Set S1
- Data Set S2

Correspondence to:
K. Kochanski,
kelly.kochanski@colorado.edu

Citation:
Kochanski, K., Anderson, R. S., & Tucker, G. E. (2018). Statistical classification of self-organized snow surfaces. *Geophysical Research Letters*, *45*, 6532–6541. https://doi.org/10.1029/2018GL077616

Received 20 FEB 2018
Accepted 1 JUN 2018
Accepted article online 7 JUN 2018
Published online 5 JUL 2018

Statistical Classification of Self-Organized Snow Surfaces

K. Kochanski[1,2,3], R. S. Anderson[1,2], and G. E. Tucker[1,3]

[1]Department of Geological Sciences, University of Colorado Boulder, Boulder, CO, USA, [2]Institute for Arctic and Alpine Research, University of Colorado Boulder, Boulder, CO, USA, [3]Cooperative Institute for Research in Environmental Sciences, University of Colorado Boulder, Boulder, CO, USA

Abstract Wind-swept snow self-organizes into bedforms. These bedforms affect local and global energy fluxes but have not been incorporated into Earth system models because the conditions governing their development are not well understood. To address this difficulty, we created statistical classifiers, drawn from 736 hr of time-lapse footage in the Colorado Front Range, that predict bedform presence as a function of wind speed and time since snowfall. These classifiers provide the first quantitative predictions of bedform and sastrugi presence in varying weather conditions. We find that the likelihood that a snow surface is covered by bedforms increases with time since snowfall and with wind speed and that the likelihood that a surface is covered by sastrugi increases with time and with the highest wind speeds. Our observations will be useful to Earth system modelers and represent a new step toward understanding self-organized processes that ornament 8% of the surface of the planet.

Plain Language Summary Wind-swept snow does not lie flat. It self-organizes and forms dunes, ripples, and anvil-shaped sastrugi. These textures cover about 8% of the surface of the Earth. They absorb more light and heat than flat snow, but they are not yet included in major climate models. We observed many fields of bedforms in the Colorado Front Range. We used these data to create and test rules that predict when snow surfaces are flat, when they form bedforms, and when they form sastrugi. These are intended to allow snow and Earth system modelers to estimate and forecast the extent of snow bedforms. We identify the wind speeds and weather variables which exert the greatest control on the shapes of snow surfaces. Snow scientists will be able to use our results to predict the behavior of wind-blown snow more reliably from less data. Finally, our results point toward the forces that which drive the self-organization of wind-blown snow, which may inspire new process-based studies of snow movement around the Earth.

1. Introduction

Snow surfaces are roughened and textured by the wind. These self-organized textures, collectively known as snow bedforms, are ubiquitous on ice sheets, on tundra, on sea ice, and in alpine regions. They cover up to 8% of the surface of the Earth (Filhol & Sturm, 2015). They are the bane of backcountry skiers and have tugged at the sleds of polar explorers since people first set foot on Antarctica.

Snow bedforms were first formally documented by Cornish (1902), who traveled 3,000 wintry miles across Canada and returned to England to craft a report titled *On Snow-waves and Snow-drifts*. As the Antarctic opened in the twentieth century, visitors remarked upon the continent's well-developed drifts and *sastrugi*, an erosional texture. Sastrugi are the most widespread snow bedform and cover much of Antarctica and Greenland. Doumani (1967) photographed sastrugi and other bedforms around Byrd Station in West Antarctica. Parish and Bromwich (1987) and Remy and Ledroit (1992) used sastrugi as lineations to map the near-surface wind field of Antarctica. Inoue (1989) observed that sastrugi on the Antarctic Plateau do not always align perfectly with the direction of the wind. They proposed that Antarctic sastrugi form mostly in summer, when the snow is relatively soft and erodible, and that in winter they are hard and resistant to changing winds. Kobayashi (1972, 1980) measured the wind speeds above bedforms near Sapporo, Japan. They studied the motion of snow ripples on underlit glass tables and saw them evolve, much like sand ripples, through a combination of saltation and creep. Most recently, Filhol and Sturm (2015) reviewed the literature on snow bedforms and presented novel light detection and ranging (LiDAR) scans of barchan snow dunes. They noted that snow dunes are smaller than sand dunes and hypothesized that the dunes grow for only 24–48 hr before they sinter and become immobile.

The last few years have brought a flurry of interest in snow bedforms. Recent researchers have worked to quantify the effects of sastrugi on surface roughness. Jackson and Carroll (1978) and Inoue (1989) observed that the greatest surface roughnesses in Antarctica occur over sastrugi fields. Vignon et al. (2017) observed that the aerodynamic roughness length perpendicular to a field of sastrugi was 100 times higher than drag parallel to them. Andreas and Claffey (1995) observed atmospheric drag change by 30% in 12 hr in response to snow redistribution. Amory et al. (2016, 2017) observed sastrugi as they adjust to changing wind direction and measured the seasonal correlation between wind drag and sastrugi size.

Sastrugi also change radiative energy fluxes into the snowpack. They decrease the albedo of snow surfaces and add uncertainty to satellite observations of the reflectivity of Antarctica (Corbett & Su, 2015; Leroux & Fily, 1998; Warren et al., 1998). Bedforms create variations in snow depth, which increase lateral heat fluxes through snow and increase its average thermal conductivity. This effect is clearly visible on sea ice, where snow dunes exert a controlling influence on heat absorption and melt pond growth (Petrich et al., 2012).

Despite the effects of sastrugi on global energy fluxes, we cannot yet predict when and where sastrugi appear. This makes it difficult to forecast their effects. At present, many major Earth system models (Vignon et al., 2018), sea ice models (Lecomte, 2014), and avalanche forecasting models (Bartelt & Lehning, 2002) treat snow as a flat layer of constant roughness.

Models that do include variable snow surface roughness elements do not fully capture the underlying snow processes. For example, the aerodynamic roughness length in the Modèle Atmosphérique Régional varies linearly with the wind speed (Gallée et al., 2015) and, in a recent update, with temperature (Agosta et al., 2018). This is a simplified representation of a snow surface. Previous authors have asserted that bedform growth is a function of wind speed (Kobayashi, 1980), snow hardness (Inoue, 1989), time (Filhol & Sturm, 2015), or temperature (Amory et al., 2017). At present, snow roughness remains the main source of uncertainty in Modèle Atmosphérique Régional estimates of blowing snow fluxes in Antarctica (Amory et al., 2015).

We present classifiers that identify the wind, time and temperature conditions that produce bedforms as opposed to flat snow surfaces. We further distinguish the conditions that produce sastrugi from those that produce other bedforms, as sastrugi have documented effects on surface roughness and energy fluxes.

2. Field Site

We observed snow bedforms on Niwot Ridge, Colorado. The site is on the downwind end of a broad, treeless 3-km-long ridge, 5 km east of the Continental Divide (Figures S1 and S2 in the supporting information). The ridge is a reliable source of snow bedforms. It receives deep, dry snowfall that is shaped by consistent westerly winds. Snow falls from October through June, with the heaviest blizzards between January and March. Each blizzard provides a blank canvas on which bedforms evolve for a few days or weeks until they are buried by the next storm.

Weather (Losleben, 2018a) and precipitation (Losleben, 2018b) data are available from the Niwot Ridge Long-Term Ecological Research Program station 200 m downwind of our cameras. Temperature measurements were collected with a Campbell Scientific CS500 mounted in a Stevenson Screen 1.5 m above ground and wind speed with an RM Young 501D mounted 7.5 m above ground. Data were recorded at 5s intervals using a Campbell Instruments CR1000 data logger. The recorded wind speeds from November to March average 10.5 m/s (23.5 mph) with occasional sustained winds as strong as 23.0 m/s (51.5 mph). Winter temperatures average −7.5 °C and vary from −28 to 11 °C. Melting temperatures occur every month.

We observed bedforms in person and through Day6 Plotwatcher Pro time-lapse cameras that took photos every 10 s during daylight hours. The cameras were active from February to March 2016 and October 2016 to March 2017. They captured a total of 736.2 hr of good visibility footage. Sample time-lapse videos are online at Kochanski (2018b), and all videos are archived in Kochanski (2018a).

3. Snow Bedform Evolution

In this section, we describe common patterns of bedform growth. We use qualitative descriptions, such as *low wind* and *fresh snow*, supplemented by measurements taken in person and references to three example blizzards (Figure 1). These descriptions foreshadow our quantitative results in section 5.

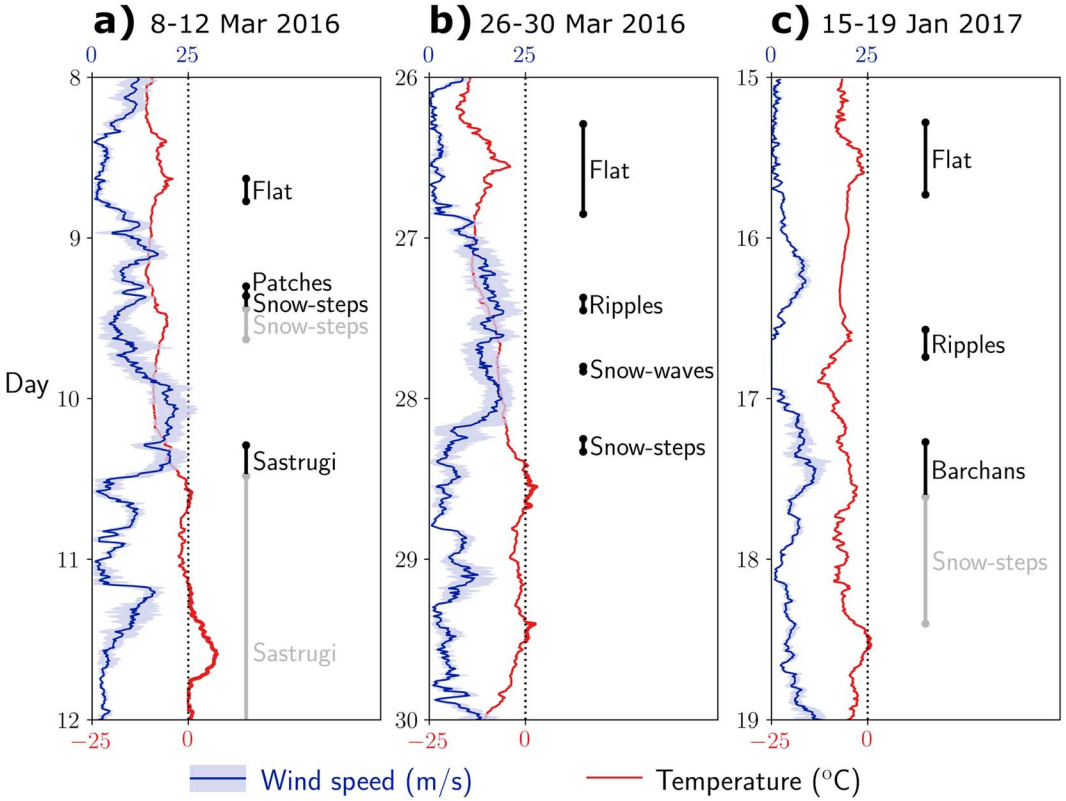

Figure 1. Evolution of the snow surface following three blizzards on Niwot Ridge. Time flows vertically. Wind speed (blue, gusts and lulls shaded) and temperature (red) vary across the horizontal. Observed surface textures are indicated in text and are missing at night and during white outs. Snow fell, in each instance, after sunset the previous night. Moving bedforms are marked in black, and bedforms not moving visibly are marked in gray.

Snow surfaces on Niwot Ridge evolved along a somewhat predictable path. At first, fresh fallen snow was dry and powdery. Snow was only flat when it fell during a period of low wind (as in Figures 1a–1c); however, these flat surfaces were short lived, like flat sand (Anderson & Haff, 1988). If snow fell during a period of higher wind, it was immediately swept into ripples or dunes. If the wind rose on an initially flat surface, the surface became roughened into ripples (e.g., Figures 1b and 1c) or dunes. We never observed a bedform-covered surface become flat, except by burial in fresh snow. Our observations indicate that flat surfaces are unstable in windy conditions and that the growth of bedforms, like many self-organized processes (England, 2015), is irreversible.

Snow became cohesive over time. Once some of the snow was solidified, the loose snow that remained formed barchan dunes, transverse snow waves, or irregular longitudinal *loose patches* (e.g., Figures 1a–1c) that migrated over the cohesive surface.

The wind carved fully solidified snow into forms that resembled scoured rock. These forms included both small *snow steps* and larger sastrugi. Snow steps appear to be an early stage of sastrugi development (Doumani, 1967) and are described in detail in section 4.1. Snow steps sometimes grew into sastrugi during periods of high wind (Figure 1a). Growth and visible movement (indicated by black/gray lines in Figure 1) stopped after a few days (Figure 1c) or after the temperature rose above freezing (Figures 1a and 1b). Most surfaces were not visibly changed by melting, although some melted and refrozen surfaces were shiny in low-angle light. In person, we found that warmed snow on Niwot Ridge was frequently soft and cohesive with no crusts or ice lenses.

Sastrugi appear to be exceptionally stable. We never saw them evolve into another bedform. During two long interstorm intervals, we saw sastrugi persist without visible motion for 11.3 and 17.5 days. We often detected buried sastrugi, both by foot and by avalanche probe, beneath one or more layers of fresh snow.

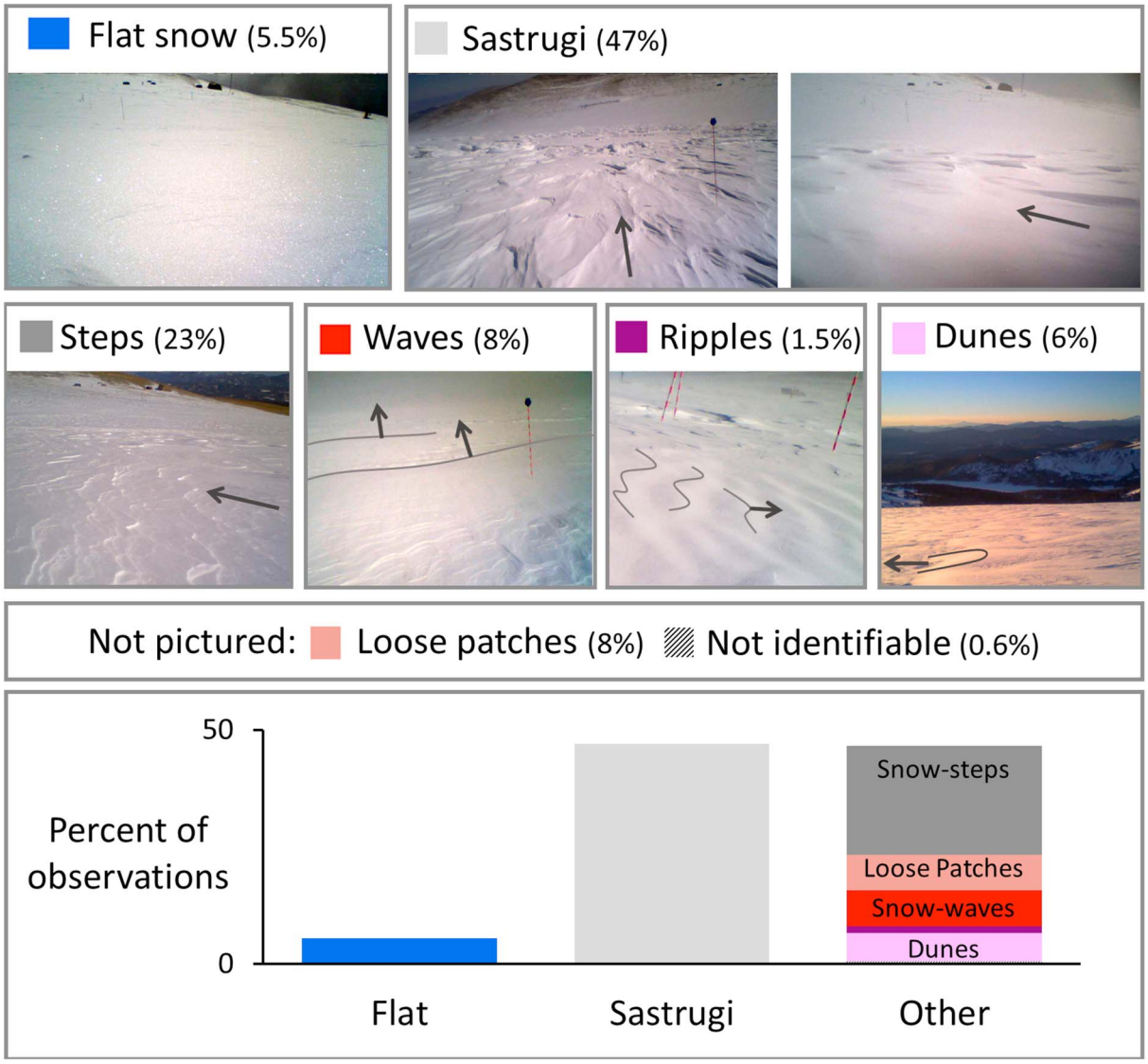

Figure 2. Bedforms of Niwot Ridge, Colorado, and frequencies of appearances in our data set. Crest motion is indicated for snow waves, dunes, and ripples. Other arrows indicate wind direction.

4. Methods

We constructed classifiers that divide the space of possible weather conditions into those that form sastrugi, those that form other bedforms, and those that leave snow flat. These classifiers are motivated by the snow surfaces we observed (section 4.1) and a set of weather variables likely to affect bedform growth (section 4.2). We constructed many softmax classifiers using combinations of these variables (section 4.3). The most powerful classifiers are presented in section 5.

4.1. Snow Surface Classification

We classify snow surfaces as flat, sastrugi, or *other bedforms*. Example images from our cameras are shown in Figure 2, and sample videos at Kochanski (2018b). Our data consist of 84 observations (Data Set S1). The relative frequency of appearance of each bedform is given in Figure 2.

Characteristics of the three bedform categories are as follows:

1. Flat snow surfaces lack sharp points, steep slopes, and movement. When fresh, they sparkle.
2. Sastrugi are erosional bedforms scoured into hardened snow. They are distinguished by regular points that face into the wind. They may retreat downwind.

3. "Other bedforms" are transient bedforms whose effects on surface energy fluxes have not yet been quantified. This category includes snow steps, snow waves, ripples, barchan dunes, and loose patches of snow.

The most difficult bedforms to distinguish were sastrugi and *snow steps*, a smaller erosional bedform with vertical edges. Snow steps lack regular points and in field observations were always smaller than 2 cm. Sastrugi were frequently 15- to 40-cm deep and spanned 45–90 cm between the points. The remaining other bedforms also tend to be smaller than sastrugi, although we have observed a few dunes and waves with crests 40- to 50-cm tall.

We excluded *not identifiable* surfaces from analysis. These are either flat surfaces or low-lying dunes, which were indistinguishable in low-contrast lighting. In contrast, the hard corners of snow steps and sastrugi are clearly visible in our footage. Our data set excludes nights, white outs, and iced-over camera lenses.

4.2. Weather Variables Tested in Classifiers

To identify variables likely to influence bedform evolution, we drew on literature from snow science and from aeolian and fluvial sediment transport.

Sastrugi appear only in cohesive snow, and thus, their appearance must correlate with snow hardening. Dry, subfreezing snow hardens as water vapor diffuses between grains (Colbeck, 1983). The rate of this process is proportional to the strength of bonds between snow grains, which Colbeck (1998) found increased with the square root of the age of the grains, $A^{0.5}$. Alternately, Filhol and Sturm (2015) used an empirical model in which hardness increases linearly with grain age, A. We calculate A as the time since snowfall, determined by the appearance of fresh snow in our footage (see section S1.1).

In wet conditions, snow grains sinter effectively instantaneously (Blackford, 2007; Colbeck, 1997). This process can be identified retrospectively by the maximum temperature T_{max} that the surface has experienced since snowfall or a binary threshold for melting, $M \equiv (T_{max} \geq -1\ ^\circ\mathrm{C})$. Finally, Amory et al. (2017) found that drag from bedforms correlated with instantaneous temperature T.

Other bedforms, such as dunes, resemble sand bedforms and are likely formed by similar aeolian processes. Many formulas exist for sand or snow grain transport by an overlying fluid moving at speed u. Most predict that transport rate should increase with the wind power, which is proportional to u^3 (see summaries for sand in Bagnold, 1941; Greeley & D'Iverson, 1985; and snow in Takeuchi, 1980). Individual grains are displaced as a result of fluid shear stress, the magnitude of which is proportional to u^2 (Bagnold, 1941). The effects of wind stress and wind power are typically controlled by a threshold above which the fluxes of grains increase nonlinearly. Li and Pomeroy (1997) give a formula for the threshold of motion, u_{crit}, of dry snow on the Canadian prairies. They give a value of 7.3 m/s at our anemometer height. We use this to define the average excess wind speed, $\overline{u_X} \equiv \overline{u - u_{crit}}$ and to calculate excess stress $\overline{u_X^2}$ and power $\overline{u_X^3}$. Finally, numerous authors since Wolman and Miller (1960) have found that geomorphic work is largely accomplished by flows that are higher than average. We capture extreme events by measuring the 90th percentile wind speed, u_{90}, that a surface has experienced since snowfall.

The forms of sand dunes depend on the wind direction θ (Werner, 1995). This may also affect the organization of snow.

To calculate these variables, we associate each event with a time of observation and a time of snowfall, separated by a period of length A. We draw wind and temperature during this period from Losleben (2018a) and calculate all averages and percentiles on that subset of the data.

Logistic regressions handle only discrete data points. Our bedform observations last minutes to weeks, however, and Front Range snowfall lasts hours to days. We therefore represent each observation with a set of Monte Carlo simulations distributed throughout the ranges of snowfall and observation times (sections S1.1 and S1.2). This method quantifies the effect of the largest source of uncertainty in our study: the uncertainty of the time snow falls. We identified snowfall events from the time-lapse imagery. This guarantees that we record only snow events that affect our field site, as precipitation in the Front Range is highly localized. Typically, the camera grays out in an afternoon storm and reveals a field of sparkling new snow the next morning. This constrains the time of snowfall to within half a day, a period of time comparable to the length of a short storm. Where the imagery is ambiguous, we constrain the snowfall period with local weather data (Losleben, 2018b).

4.3. Softmax Classifiers: Construction, Comparison, and Validation

We used softmax classifiers, also known as logistic regression models, to predict bedform type as a function of the many weather-related variables described above. Softmax classifiers are the standard method for separating discrete classes of data and are reviewed in many textbooks and papers (e.g., Bewick et al., 2005; sections S1.3 and S1.4). Much as linear regression identifies the line that best follows the trend of one group of data points, logistic regression identifies the line or plane that best separates two groups of data points.

We constructed softmax classifiers using all possible combinations of one, two, or three of the weather variables above and searched for the models with the most predictive power. We excluded models that included both A and its square root $A^{0.5}$. The results shown in section 5.1 are therefore the best of 460 models.

Predictive equations of many variables tend to fit data well but have little explanatory power; therefore, we identify the classifiers that generate the best predictions from the fewest number of variables. We penalized models that used more variables using log-likelihood ratios (section S1.5). We validated each result using bootstrapping, a method for testing the sensitivity of a data set to outliers (Efron, 1981; section S1.6).

5. Results

5.1. Best Snow Surface Classifiers

The effects of time and temperature on bedforms are shown in Figures 3a and 3b. The best of the 460 classifiers we tested are shown in Figures 3c and 3d and discussed below.

Flat snow surfaces were consistently associated with fresh snow (low age A) and low winds (u). The best classifier for bedform presence was as follows:

$$\frac{u}{u_f} \leq \left(1 - \frac{A}{A_f}\right) \Longrightarrow P(\text{flat}) \geq P(\text{bedforms}), \tag{1}$$

where $u_f = 6.4 \pm 2.2$ m/s and $A_f = 1.42 \pm 0.33$ days. This is the equation of the line in Figure 3c. This classifier had a total accuracy of 99% on our validation data set, with a 10% false positive and 0.6% false negative rate.

Sastrugi tend to appear on older snow that has experienced high wind speeds. Their presence was best predicted by the age of the snow grains A and the 90th percentile wind speed since snowfall u_{90}.

$$\frac{u_{90}}{u_s} \geq \left(1 - \frac{A}{A_s}\right) \Longrightarrow P(\text{sastrugi}) \geq P(\text{not sastrugi}), \tag{2}$$

where $u_s = 29.70 \pm 0.13$ m/s and $A_s = 10.32 \pm 0.24$ days. This equation is presented visually in Figure 3d. This classifier had a total accuracy of 84%, with a 16% false positive rate and 21% false negative rate.

The negative slopes of equations (1) and (2) are mathematically inevitable. Flat surfaces can grow bedforms, but bedforms cannot become flat. Therefore, old flat surfaces must be less common than young flat surfaces. Likewise, sastrugi are more common on old surfaces than young ones because they do not devolve into other bedforms.

Our classifiers predicted flat surfaces more reliably than sastrugi-covered surfaces (see L in Table 1). We expect that high-accuracy prediction of sastrugi presence will require a complex model, as sastrugi grow out of transient bedforms that are shaped by multiple processes. Equation (2) is the most accurate classifier that does not require a detailed knowledge of the surface history.

5.2. Variables That Predict Bedform Presence

In this section we discuss the performance of each variable in our classifiers. We summarize all single-variable classifiers in Table 1 and present the full results in Data Set S2. Where our results disagree with previous studies, we identify physical processes that could explain our observations.

Bedforms and sastrugi appear linearly in time (Figure 3a). In all classifiers tested, A was a slightly better predictor of bedform presence than $A^{0.5}$. This is an unexpected result: Older surfaces must grow bedforms more easily than fresh ones. If flat surfaces turned into bedforms at a constant rate, the fraction of flat surfaces would decrease exponentially in time. This disagrees with the hypothesis by Filhol and Sturm (2015), who predicted that old snow surfaces would change less easily than young ones, as older surfaces would be harder and have a higher threshold for motion. These results allow two explanations. It is possible that erosive snow bedforms, like snow steps, grow faster than granular bedforms like ripples. Alternately, it is possible that flat surfaces

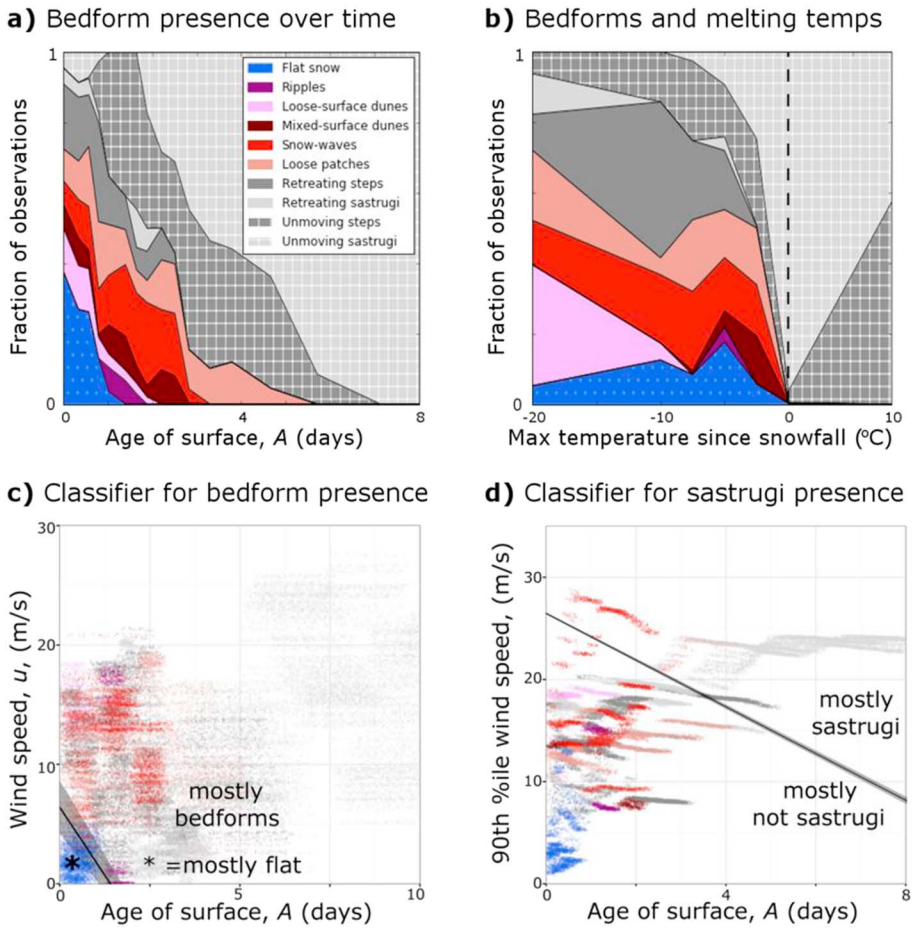

Figure 3. Bedforms on Niwot Ridge at various snow grain ages (a), temperatures (b), wind speeds (c), and 90th percentile wind speeds (d) Bedforms are color coded; see legend in plot (a). *Unmoving* bedforms do not move visibly in our footage. Plots (a) and (b) are one-variable frequency diagrams showing how the occurrence of various bedforms varies with the age of the snow grains and highest temperature experienced on the surface. Plots (c) and (d) are two-variable scatter plots. The lines mark the best classifiers to divide (c) flat surfaces from bedform-covered surfaces and (d) sastrugi-covered from nonsastrugi covered surfaces. Classifier uncertainties are shaded gray. Monte Carlo simulation multiplied the number of data points (section S1.4).

on Niwot Ridge never persist long enough to harden substantially. Our site was chosen for strong, regular winds. Perhaps A_f is the time constant for bedform growth under the site's gentlest winds.

The rate of formation of sastrugi also increases as the snow ages. Again, this is clear because the best sastrugi classifier is linear in time (equation (2)), though the data are noisier (compare fits of lines in Figures 3c and 3d). This is expected, as sastrugi form only in hardened snow, but we were surprised that our data did not align with a known timescale for sintering. Snow usually hardens within 24–48 hr (Bromwich et al., 1990; Mather, 1962), yet we saw dunes and snow waves moving 48–72 hr after snowfall.

We hypothesize that snow dunes and waves are part of a negative feedback that inhibits sastrugi growth. When sastrugi start to grow, the surface is eroded, and snow particles are released onto the surface. The loose grains self-organize into waves or dunes. These dunes cover parts of the surface, preventing further erosion, and may fill in the sastrugi.

Wind speed was an important predictor for both bedform and sastrugi presence. Flat surfaces were best predicted by instantaneous wind speed u, followed by linearly averaged winds ($\overline{u}$). The wind speed variables without thresholds performed better than those with thresholds. This implies that bedform initiation is a linear, threshold-free process. Freshly fallen snow contains some very small particles, and we expect that these may be disturbed even by very gentle winds.

Table 1
Performance of Selected Models of Bedform Presence (Flat/Not) and Sastrugi Presence (Sastrugi/Not) on the Surface of Niwot Ridge

		Flat/not		Sastrugi/not	
Weather variable(s) in classifier		*L*	Dir	*L*	Dir
Single-variable classifiers					
β_0	Constant value (ignores all weather)	−22	–	−55	–
A	Age of snow grains	−14	–	−56	+
$A^{1/2}$	Square root of age	−19	–	−57	+
u	Instantaneous wind speed	−12	–	−57	+
$\overline{u}$	Average wind speed	−13	–	−58	+
$\overline{u^2}$	Average of wind speed squared	−11	–	−58	+
$\overline{u^3}$	Average of wind speed cubed	−12	–	−58	+
$\overline{u_X}$	Average excess wind speed	−13	–	−59	+
$\overline{u_X^2}$	Average of excess wind speed squared	−12	–	−59	+
$\overline{u_X^3}$	Average of excess wind speed cubed	−13	–	−58	+
u_{90}	90th percentile wind speed	−13	–	−57	+
T	Instantaneous temperature	−32	+	−56	+
T_{max}	Highest temperature	−54	+	−47	+
M	Has surface warmed above −1° ?	−36	–	−60	+
θ	Instantaneous wind direction	−94	W	−93	SW
$\overline{\theta}$	Average wind direction	−93	SW	−93	E
Selected multivariable classifiers					
u, β_0, A	Best classifier for flat surfaces	−3.1		−32	
$u, \beta_0, A^{0.5}$,	Runner-up for flat surfaces	−3.6		−33	
u_{90}, β_0, A	Best classifier for sastrugi	−6		−28	
$u_{90}, \beta_0, A^{0.5}$	Runner-up for sastrugi	−7		−29	

Note. Less-negative variables of log-likelihood (*L*) indicate better model performance; differences ≥1 are statistically significant. *Dir* indicates correlation direction (compass directions for circular variables). Averages and percentiles are calculated since snowfall. Excess wind speed $u_X = u - u_{crit}$, where $u_{crit} = 7.3$ m/s.

Sastrugi presence, in contrast, was best predicted by nonlinear wind speed variables (Table 1). This shows that sastrugi growth is disproportionately controlled by high winds. The best predictor was the magnitude of the highest wind u_{90}. As highest winds increase monotonically in time, it is impossible for any surface that once passed the threshold to fall back below it. Once formed, sastrugi persist.

Maximum temperature was a useful single-variable predictor of sastrugi presence (Table 1) but performed poorly in multivariable classifiers. Melt (*M*) was similar but less effective. It is clear that melting and refreezing harden snow and promote the growth of erosive bedforms (Figure 3b), but this process is not common enough in our data to appear frequently in our classifiers. The instantaneous temperature *T* was a very ineffective predictor, as sastrugi form gradually over time.

The wind direction did not correlate with bedform presence. Wind direction affects the orientation of bedforms (Amory et al., 2016; Parish & Bromwich, 1987), but their growth is controlled by the wind speed. Temperature affected bedforms only when freezing occurred (Figure 3b).

6. Discussion

The above results provide a statistically rigorous description of bedform appearance on Niwot Ridge, Colorado. We collected 736.2 hr of time-lapse footage of evolving snow surfaces. We used this data set to construct classifiers that explore the 15-dimensional space spanned by the weather variables listed in Table 1 and that predict the conditions for bedform growth (equations (1) and (2)).

Our results make it possible for researchers to forecast the extent of snow bedforms in any site for which they have wind and snowfall data. As these data are available for much of the present Earth from weather stations,

for the past from reanalysis data, and for the future from Earth system models, our results are intended to be applied and validated worldwide. Researchers who have direct observations of snow bedforms may apply the forms of our classifiers (equations (1) and (2) and fit our parameters A_f, u_f, A_s, and u_s to their data. Researchers without observations of the snow surface may use equations (1) and (2) directly. They should be aware that parameters A_f, u_f, A_s, and u_s will only be roughly accurate for locations beyond the Front Range.

As this study is the first of its kind, we restricted our time-lapse data collection to a single site with the following distinctive weather patterns. First, Front Range blizzards are heavy. Most storms completely bury old bedforms. This allows us to ignore the history of the surface before the most recent snowfall. Bedforms in regions with light snowfall, in contrast, are built up over many storms (Filhol & Sturm, 2015). Second, the winter winds in the Front Range are unidirectional. We will not see features like star dunes, which form when wind transports sand from multiple directions (Werner, 1995). Third, the cameras were at an elevation of 3,527 m. The stress exerted by wind of a given speed will be 34% lower than that exerted by denser air at sea level. Fourth, Niwot Ridge has loose, dry snow that will sublime faster and sinter more slowly than snow in a more humid climate. Fifth, our site is located at the downwind end of a 2.5-km snow-covered ridge. This gives blown snow grains a long range over which to become rounded and sorted by the wind. The ridge also supplies wind-blown snow for several days after snow fall.

Finally, our results are intended to inspire and accelerate ongoing studies of snow bedform dynamics. We present novel observations and descriptions of snow surface evolution (section 3). Our statistical results also led to a number of hypotheses concerning snow bedform growth (section 4.2). These hypotheses will motivate process-based studies of self-organization in cohesive materials.

Acknowledgments
This research was supported by a Department of Energy Computational Science Graduate Fellowship (DE-FG02-97ER25308), by a University of Colorado Chancellor's Fellowship, and by the National Science Foundation via support for the Boulder Creek Critical Zone Observatory (EAR-1331828). Field equipment was funded by the American Alpine Club, the Colorado Scientific Society, and a Patterson Award from the University of Colorado Department of Geological Sciences. Field assistants were funded by the University of Colorado Undergraduate Research Opportunities Program. Logistical support and climate data were provided by the NSF-supported Niwot Ridge Long-Term Ecological Research Project and the University of Colorado Mountain Research station. We thank Irina Overeem, Gage Hamel, James Logan, and Richard Barnes for help in the field. We extend warm thanks to Clea Bertholet for extended field assistance and preliminary data processing. We are grateful for Matthew Sturm and Simon Filhol's enlightening comments on the nature of snow bedforms, to Gregory Kochanski for a propitious conversation about statistics, and to two anonymous reviewers for comments that improved and clarified this manuscript.

References

Agosta, C., Amory, C., Kittel, C., Orsi, A., Favier, V., Gallée, H., et al. (2018). Estimation of the Antarctic surface mass balance using MAR (1979–2015) and identification of dominant processes. *The Cryosphere Discussions*. https://doi.org/10.5194/tc-2018-76

Amory, C., Gallée, H., Vincent, F. N.-b., Vignon, E., Picard, G., Trouvilliez, A., et al. (2017). Seasonal variations in drag coefficient over a sastrugi-covered snowfield in coastal East Antarctica. *Boundary-Layer Meteorology*, *164*(1), 107–133. https://doi.org/10.1007/s10546-017-0242-5

Amory, C., Naaim-Bouvet, F., Gallée, H., & Vignon, E. (2016). Brief communication: Two well-marked cases of aerodynamic adjustment of sastrugi. *The Cryosphere*, *10*, 743–750. https://doi.org/10.5194/tcd-9-6003-2015

Amory, C., Trouvilliez, A., Gallée, H., Favier, V., Naaim-Bouvet, F., Genthon, C., et al. (2015). Comparison between observed and simulated aeolian snow mass fluxes in Adélie Land, East Antarctica. *The Cryosphere*, *9*(4), 1373–1383. https://doi.org/10.5194/tc-9-1373-2015

Anderson, R. S., & Haff, P. K. (1988). Simulation of eolian saltation. *Science*, *241*(4867), 820–823. https://doi.org/10.1126/science.241.4867.820

Andreas, E. L., & Claffey, K. J. (1995). Air-ice drag coefficients in the western Weddell Sea 1. Values deduced from profile measurements. *Journal of Geophysical Research*, *100*(C3), 4821–4831. https://doi.org/10.1029/94JC02015

Bagnold, R. A. (1941). *The physics of blown sand and desert dunes*. London: Methuen.

Bartelt, P., & Lehning, M. (2002). A physical SNOWPACK model for the Swiss avalanche warning Part I: Numerical model. *Cold Regions Science and Technology*, *35*(3), 147–167. https://doi.org/10.1016/S0165-232X(02)00073-3

Bewick, V., Cheek, L., & Ball, J. (2005). Statistics review 14: Logistic regression. *Critical Care*, *9*(1), 112–118. https://doi.org/10.1186/cc3045

Blackford, J. R. (2007). Sintering and microstructure of ice: A review. *Journal of Physics D: Applied Physics*, *40*(21), R355–R385. https://doi.org/10.1088/0022-3727/40/21/R02

Bromwich, D. H., Parish, T. R., & Zorman, C. A. (1990). The confluence zone of the intense katabatic winds at Terra Nova Bay, Antarctica, as derived from airborne sastrugi surveys and mesoscale numerical modeling. *Journal of Geophysical Research*, *95*(D5), 5495–5509. https://doi.org/10.1029/JD095iD05p05495

Colbeck, S. C. (1983). Theory of metamorphism of dry snow. *Journal of Geophysical Research*, *88*(C9), 5475–5482. https://doi.org/10.1029/JC088iC09p05475

Colbeck, S. C. (1997). A review of sintering in seasonal snow (CRREL Report, 97 (10)).

Colbeck, S. C. (1998). Sintering in a dry snow cover, *84*(8), 4585–4589. https://doi.org/10.1063/1.368684

Corbett, J., & Su, W. (2015). Accounting for the effects of sastrugi in the CERES clear-sky Antarctic shortwave angular distribution models. *Atmospheric Measurement Techniques*, *8*(8), 3163–3175. https://doi.org/10.5194/amt-8-3163-2015

Cornish, V. (1902). On snow-waves and snow-drifts in Canada, with notes on the "snow-mushrooms" of the Selkirk Mountains. *The Geographical Journal*, *85*(4), 342–365. https://doi.org/10.2307/1774538

Doumani, G. A. (1967). Surface structures in snow. In *International conference on low temperature science: Physics of snow and ice* (pp. 1119–1136). Hokkaido, Japan: Hokkaido University.

Efron, B. (1981). Nonparametric estimates of standard error: The jacknife, the bootstrap and other methods. *Biometrika*, *68*(3), 589–599. https://doi.org/10.1093/biomet/68.3.589

England, J. L. (2015). Dissipative adaptation in driven self-assembly. *Nature Nanotechnology*, *10*(11), 919–923. https://doi.org/10.1038/nnano.2015.250

Filhol, S., & Sturm, M. (2015). Snow bedforms: A review, new data, and a formation model. *Journal of Geophysical Research: Earth Surface*, *120*, 1645–1669. https://doi.org/10.1002/2015JF003529

Gallée, H., Preunkert, S., Argentini, S., Frey, M. M., Genthon, C., Jourdain, B., et al. (2015). Characterization of the boundary layer at Dome C (East Antarctica) during the OPALE summer campaign. *Atmospheric Chemistry and Physics*, *15*(11), 6225–6236. https://doi.org/10.5194/acp-15-6225-2015

Greeley, R., & D'Iverson, J. (1985). Physics of particle motion. In *Wind as a geological process* (pp. 67–107). Cambridge, UK: Cambridge University Press.

Inoue, J. (1989). Surface drag over the snow surface of the Antarctic Plateau 1. Factors controlling surface drag over the katabatic wind region. *Journal of Geophysical Research*, *94*(D2), 2207–2217. https://doi.org/10.1029/JD094iD02p02207

Jackson, B. S., & Carroll, J. J. (1978). Aerodynamic roughness as a function of wind direction over asymmetric surface elements. *Boundary-Layer Meteorology1*, *14*(3), 323–330.

Kobayashi, D. (1972). Studies of snow transport in low-level drifting snow. *Contributions from the Institute of Low Temperature Science*, *A24*, 1–58.

Kobayashi, S. (1980). Studies on interaction between wind and dry snow surface. *Contributions from the Institute of Low Temperature Science*, *A29*, 1–64.

Kochanski, K. (2018a). Time-lapse observations of snow bedforms in the Colorado Front Range, 2016–2017. Dataset on Zenodo https://doi.org/10.5281/zenodo.1253725

Kochanski, K. (2018b). Example time-lapse videos of snow bedforms in the Colorado Front Range. Retrieved from https://www.kochanski.org/kelly/snow-bedforms-in-the-colorado-front-range/

Lecomte, O. (2014). Influence of snow processes on sea ice: A model study (PhD thesis). Université Catholique de Louvain. https://doi.org/10.1017/CBO9781107415324.004

Leroux, C., & Fily, M. (1998). Modeling the effect of sastrugi on snow reflectance. *Journal of Geophysical Research*, *103*(98), 25,779–25,788.

Li, L., & Pomeroy, J. W. (1997). Estimates of threshold wind speeds for snow transport using meteorological data. *Journal of Applied Meteorology*, *36*(3), 205–213. https://doi.org/10.1175/1520-0450(1997)036<0205:EOTWSF>2.0.CO;2

Losleben, M. (2018a). Precipitation data for Saddle chart recorder from 1981-7-31 to ongoing, daily.

Losleben, M. (2018b). Climate data for Saddle data loggers (CR23X and CR1000) from 2000-6-24 to ongoing, daily.

Mather, K. B. (1962). Further observations on sastrugi, snow dunes and the pattern of surface winds in Antarctica. *Polar Record*, *11*(71), 158–171. https://doi.org/10.1017/S0032247400052888

Parish, T. R., & Bromwich, D. H. (1987). The surface windfield over the Antarctic ice sheets. *Nature*, *328*(2), 51–54.

Petrich, C., Eicken, H., Polashenski, C. M., Sturm, M., Harbeck, J. P., Perovich, D. K., & Finnegan, D. C. (2012). Snow dunes: A controlling factor of melt pond distribution on Arctic sea ice. *Journal of Geophysical Research*, *117*, C09029. https://doi.org/10.1029/2012JC008192

Remy, F., & Ledroit, M. (1992). Katabatic wind intensity and direction over Antarctica derived from scatterometer data. *Geophysical Research Letters*, *19*(10), 1021–1024.

Takeuchi, M. (1980). Vertical profile and horizontal increase of drift-snow transport. *Journal of Glaciology*, *26*(94), 481–492.

Vignon, E., Genthon, C., Barral, H., Amory, C., Picard, G., Gallée, H., et al. (2017). Momentum- and heat-flux parametrization at Dome C, Antarctica: A sensitivity study. *Boundary-Layer Meteorology*, *162*(2), 341–367. https://doi.org/10.1007/s10546-016-0192-3

Vignon, E., Hourdin, F., Genthon, C., Van de Wiel, B. J. H., Gallée, H., Madeleine, J.-B., & Beaumet, J. (2018). Modeling the dynamics of the atmospheric boundary layer over the Antarctic plateau with a general circulation model. *Journal of Advances in Modeling Earth Systems*, *10*, 98–125. https://doi.org/10.1002/2017MS001184

Warren, S. G., Brandt, R. E., & O'Rawe Hinton, P. (1998). Effect of surface roughness on bidirectional reflectance of Antarctic snow. *Journal of Geophysical Research*, *103*(E11), 25,789–25,807. https://doi.org/10.1029/98JE01898

Werner, B. T. (1995). Eolian dunes: Computer simulations and attractor interpretations. *Geology*, *23*, 1107–1110. https://doi.org/10.1130/0091-7613(1995)023<1107:edcsaa>2.3.co;2

Wolman, M. G., & Miller, J. P. (1960). Magnitude and frequency of forces in geomorphic processes. *The Journal of Geology*, *68*(1), 54–74. https://doi.org/10.1086/626637